Reliability Analysis and Life Cycle Costing Of Rehabilitation Strategies for RC Structures Exposed To Marine Environment

Hilyati B. Sabtu & Mark G. Stewart
Centre for Infrastructure Performance and Reliability, The University of Newcastle, Australia

ABSTRACT: This paper presents a reliability analysis to predict the probability of corrosion damage and to improve the management of RC structures particularly located in marine environments. The reliability analysis incorporates deterioration models, spatial variability, random field analysis, rehabilitation strategies and life-cycle costing. This study focus only on chloride-induced cracking as the corrosion due to the chloride penetration could possibly cause severe cracking at concrete surfaces. This study was aim to improve the existing crack propagation models by conducting accelerated corrosion tests for transverse reinforcement, to model the spatial variability of RC columns by using non-stationary random field analysis and to estimate the life cycle costing of rehabilitation strategies for evaluating the economic performance of 24 repair alternatives related to chloride-induced corrosion problem. The incorporation of the reliability analysis with the life cycle costing of rehabilitation strategies have a potential to be a massive contribution for decision makers, asset owners and engineers to control the initial, present and future cost of assets ownership. In order to improve the existing crack propagation models, the accelerated corrosion tests are undertaken in two stages; the first stage which has been completed was focused on the effect of reinforcement confinement (including transverse reinforcement) and spacing of reinforcing bars on concrete cover cracking and the second stage will be conducted to improve the existing crack propagation models in order to provide more realistic results. In this paper, results from the first stage of accelerated corrosion tests are presented and results revealed that confinement and spacing of reinforcing bars have a significant effect on the rate of crack propagation.

1 INTRODUCTION

Corrosion of steel in concrete is a worldwide issue affecting the durability of RC structures, particularly for RC structures located in marine environments. Steel bars are naturally protected against corrosion by passivation of steel surface due to the high alkalinity of the concrete. The corrosion begins when a sufficient amount of chlorides penetrate into a concrete cover and destroy the inhibitive property by permeating the passivating layer of steel surface and increase the risk of corrosion. Once the corrosion propagates, the corrosion products create an expansive pressure on the surrounding concrete which causes concrete cover cracking (Zhao et al. 2012). Corrosion-induced cover cracking is an important measure for evaluating the service life of RC structures. The deterioration due to chloride-induced cover cracking leads to structural failure and reduces the service life of RC structure (Zhong et al. 2010). For these reasons chloride-induced cover cracking becomes a significant concern to asset owners. Structures suffering from chloride-induced cover cracking require high frequency of site investigation, repair, maintenance and rehabilitation work as it demands large expenditure from asset owners.

The chloride-induced cover cracking process is best described in three phases: (i) the corrosion initiation phase is the time it takes for chloride ions to penetrate the concrete cover; (ii) the crack initiation phase is the time it takes from corrosion initiation to when visible crack width appears; (iii) and the crack propagation phase is the time it takes from when a visible crack appears to when the crack reaches a limit crack width (Stewart & Mullard 2007). A common method of estimating the rate of chloride ingress into reinforced concrete structure is by the use of Fick's 2nd Law of non-stationary diffusion. The rate of transfer, J of diffusing chloride ion through a plan perpendicular to the direction of diffusion is assumed proportional to the concentration gradient and for 1-dimensional flow in a semi-finite solid the diffusion rate is given as:

$$J = \frac{\partial C(X)}{\partial t} = D_c \frac{\partial^2 C(x)}{dx_1^2} \quad (1)$$

where J is the rate of chloride ion diffusion through a plane perpendicular to the direction of diffusion, C(x) is the chloride concentration at a distance x

from the surface and D_c is the chloride diffusion coefficient. The equation of diffusion above can be solved for several sets of initial conditions. The chloride concentration C(x,t) at a distance x from a concrete surface at time t is

$$C(x,t) = C_0 \left[1 - \mathrm{erf}\left(\frac{x}{2\sqrt{D_c t}}\right)\right] \quad (2)$$

where C is the chloride concentration at a distance x from the surface at time t years, C_0 is the surface chloride concentration, D_c is the chloride diffusion coefficient and erf is the error function. The Equation 2 above is given empirically by Fick's second law of diffusion. However, based on study done by Val & Stewart (2003), chloride penetration process and field conditions are found dissimilar from assumption of Fick's Law. An improved model utilising a time-dependent chloride diffusion coefficient proposed by DuraCrete (1998) are as follows:

$$C(x,t) = C_0 \left[1 - \mathrm{erf}\left(\frac{x}{2\sqrt{k_e k_t k_c D_c \left({}^{t_0}/_{t}\right)^{n}(t)}}\right)\right] \quad (3)$$

Equation 3 is used to determine the chloride content at distance x, in time t, by the theory of diffusion. C_0 is the surface chloride concentration. Three environmental factors have proposed by DuraCrete (1998) need to be quantified statistically which is K_e is the environment factor, K_t is the test method factor and K_c is the curing factor. Where D_c is the apparent chloride diffusion, n is the age factor, T is the exposure period in year and to be the reference period in year (28days or 0.0767).

For estimating the initial corrosion rate at the start of corrosion propagation and the time-variant corrosion rate have been proposed by Vu and Stewart (2005). The corrosion rate at the time of initiation can be calculated as a function of the water/cement ratio and concrete cover as:

$$i_{corr}(1) = \frac{27(1-w/c)^{-1.64}}{C} \quad (4)$$

where i_{corr} (1) is the corrosion rate for the first year in $\mu A/cm^2$, w/c is the water cement ratio and C is the concrete cover in mm. The time-variant corrosion rate can be described as:

$$i_{corr}(t_p) = i_{corr}(1) \cdot 0.85 t_p^{-0.29} \qquad t_p > 1 \text{ year} \quad (5)$$

where t_p is the time since corrosion initiation in years and i_{corr} (1) is the corrosion rate for the first year in $\mu A/cm^2$. Crack initiation model in this study will use a model proposed by El-Maaddawy & Soudki Model (2007). Crack initiation can be calculated as:

$$t_{1st} = \left[\frac{7117.5(D+2d_0)(1+v_c+)}{i_{corr}E_{ef}}\right]\left[\frac{2cf_t}{D} + \frac{2d_0E_{ef}}{(1+v_c+)(D+2d_0)}\right] \quad (6)$$

where t_{1st} is time from corrosion initiation to first cracking, D is the reinforcing bar diameter (mm), d_0 is the thickness of the porous zone around the reinforcing bar (μm), $\square_c$ is the Poisson's ratio of concrete, C is the concrete cover (mm), f_t is the design concrete tensile strength (MPa), i_{corr} is the current density ($\mu A/cm^2$) and E_{ef} is the effective elastic modulus of concrete defined as:

$$E_{ef} = {}^{E_c}/_{(1+\emptyset_{cr})} \quad (7)$$

where E_c is the elastic modulus of concrete (MPa) and $\emptyset_{cr}$ is the concrete creep coefficient. Ψ is defined as:

$$= {}^{D'^2}/_{2C(C+D')} \quad (8)$$

$$\text{where } D' = D + 2d_0 \quad (9)$$

The El-Maadway and Soudki (2007) model accounts for concrete cover, concrete strength, bar diameter and the effect of the porous zone at the steel/concrete interface. The advantages of this model are that provides quick, robust and accurate mathematical estimation of the time from corrosion initiation to the time of first cracking.

The most recent crack propagation Model studied by Mullard & Stewart (2011) involved four series of reinforced concrete slabs to investigate the relative influence of concrete cover, concrete strength, bar diameter and bar confinement on the rate of crack propagation for one way slab. The time to severe cracking to reach a limit crack width (W_{lim}) is

$$t_{sp} = t_{1st} + k_R \frac{w_{lim}-0.05}{k_c r_{crack}}\left(\frac{0.0114}{i_{corr}}\right) \quad (10)$$

$$\text{where } r_{crack} = 0.0008e^{-1.7016\Psi_{cp}} \quad (11)$$

$$0.1 \leq {}_{cp} \leq 1.03 - 10 \quad (12)$$

where t_{sp} is the time taken from corrosion initiation to severe cracking (years); k_c is the confinement correction factor and if reinforcing bar is in internal location, than k_c is equal to unity; k_R is the rate of loading correction factor; w_{lim} is the limit crack width that define the excessive cracking (mm); r_{crack} is the rate of crack propagation that can obtained from Equation 11.

Many empirical studies have been conducted to investigate the crack initiation and propagation phases (e.g., Andrade et al. 1993; Liu & Weyers 1998; Alonso et al. 1998; Vu et al. 2005). During the crack initiation phase, the time to crack initiation is much lesser compared to the time to crack propagation. Mullard & Stewart (2011) discovered that the

accuracy of a model for crack initiation will not significantly affect the timing of corrosion damage for RC structures. Considering crack initiation as the end of service life of structures is too conservative as the formation of cracks approximately 0.05 mm are very small and do not affect the serviceability of structures. Hence, understanding and modelling the crack propagation phase is the main area of future study.

To date, there are limited numbers of studies in the literature on crack propagation based on empirical methods (Andrade et al. 1993, Liu & Weyers 1998, Alonso et al. 1998, Vu et al. 2005, Mullard & Stewart 2011). These experiments have some limitations in terms of parameters, lack of practicability and some experiments were unrealistic due to idealised geometries of specimens. Therefore, more research should be conducted to study crack propagation in order to improve existing crack propagation models. This paper describes the effect of reinforcement confinement (and transverse reinforcement) and spacing of reinforcing bars in the crack propagation phase on RC slab specimens.

2 RESEARCH SIGNIFICANCE

2.1 *Empirical method on crack propagation*

Numerous studies have been conducted using non-destructive methods to study the corrosion process; however it is impossible to accurately evaluate the corrosion distribution along the reinforcing bars in-situ with the concrete cover. Hence, some experimental work based on accelerated corrosion tests or natural corrosion processes have been carried out in order to study the empirical link between the occurrence and widths of cracks and the amount of corrosion (Zhang et al. 2010).

The use of accelerated corrosion testing in the laboratory has become the most common technique to speed up the corrosion-induced damage in reinforced concrete structures. Studies done by Val et al. (2009) stated that the accelerated corrosion test provides data on crack growth based on the amount of corrosion (for example, Maruyama et al. 1989; Andrade et al. 1993; Cabrera 1996; Rodriguez et. al 1996; Alonso et al. 1998; Mangat & Elgarf 1999; Vu et al. 2005). An empirical study by Vidal et al. (2004) found formulas relating the crack width with the amount of corrosion (Val et al. 2009). Field studies suggested that the use of empirical models to study the crack propagation phase is computationally fast, relatively accurate prediction for cracking times based on input parameters that are readily available (Mullard & Stewart 2011).

2.2 *Limit crack width*

The maximum crack width is an indication of the end of service life for RC structures. If cracks that appear on the concrete surface are too wide, it will destroy the aesthetic of the structures and reduce the serviceability of such structures. Several codes and standards can be referred as a guideline to ensure that a certain crack width might not impair the appearance of a structure and also do not reduce the serviceability or durability performance of a structure (ACI Committee 224 2001, Norwegian standard NS 3474 E 1992 and Canadian Offshore Code CSA-S474-04 2004). However, the guides recommend that the permissible crack widths are due to the service loads.

For crack width due to chloride penetration, certain limit crack widths have been proposed, for example, Vu & Stewart (2005) and Mullard & Stewart (2011). Research done by Mullard & Stewart (2011) stated limit crack widths defined by other researchers. For example, limit crack width between 0.15 and 0.4 mm is appropriate for durability or aesthetic limit states (Andrade et al. 1993, ACI Committee 224 2001) and limit crack width of 0.8 mm is appropriate for aesthetic requirements (Sakai et al. 1999).

As the definition of limit crack width is unclear and repeatedly receiving debates and discussions, therefore limit crack width has been investigated under Public Work Department (PWD) of Malaysia policies. Although there is no specification on maximum allowable crack width for cracking due to chloride penetration, however cracks below 1.0 mm is categorised as hairline cracks. If hairline cracks were found, it is necessary to record the condition for observation purposes. Crack width of 1.0 mm is defined as the limit for aesthetic and serviceability. The PWD of Malaysia (2006) recommended that crack width between 1.0 to 5.0 mm is severe cracking; therefore it is necessary to implement repair and maintenance work.

2.3 *Confinement and spacing of reinforcing bars*

Reinforcement confinement refers to the volume of concrete surrounding the reinforcing bars that has an effect on crack propagation. Mullard & Stewart (2011) discovered that the cracks over the reinforcing bars located at the edge of specimen have a higher propagation rate than the cracks over the reinforcing bars located at the internal positions. The internal bars having a larger area of confinement and spacing of reinforcing bars have greater capacity to resist the tensile stress. Figure 1 shows a schematic of the effect of reinforcement confinement on crack width. This phenomenon is rarely mentioned in the literature, and the Mullard & Stewart (2011) study was based on experimental data for one-way RC slabs. Therefore, further study is conducted to pro-

vide more robust and realistic results due to this structural behaviour by examining crack behaviour for two-way slabs (ie. transverse reinforcement).

Typical spacing of reinforcing bars for bridges and buildings is between 100 mm to 300 mm as recommended in British Standard 8110 (Code of Practise for Design and Construction 1997). The decision of selecting the appropriate spacing reinforcing bars is generally based on design experience, engineering judgement and economic considerations. Investigation on the effect of spacing of reinforcing bars will contribute an understanding and awareness for engineers and designers in their decision making while selecting the right measurement for spacing of reinforcing bars specifically to the RC structures located in marine environments. Therefore spacing of reinforcing bars is another parameter to be investigated in this study.

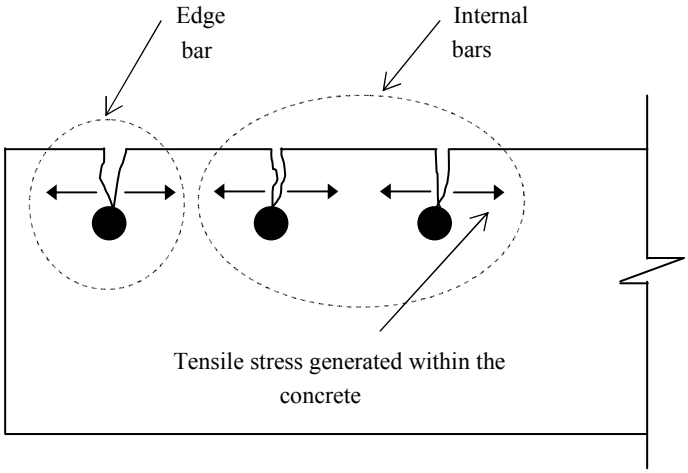

Figure 1. Effect of reinforcement confinement on crack width.

2.4 Random Field Analysis

A homogeneous analysis can lead to underestimation the probabilities of failure. Therefore, in this study, random variability is to be considered on the variation across samples and variation over space. The variables are not concentrated only at a particular location but they are distributed in space. Random field is considered as a surface of a reinforced concrete structure then the surface is divided into an appropriate number of small sizes by using midpoint method. By using midpoint method, random field within an element is represented by a value at the centroid of each element and for stationary random field analysis, this value is assumed to be constant within elements. Each of the random variables within the random field is statistically correlated based on the correlation function of the corresponding random field. Random field is defined by its mean (μ), standard deviation (σ) and correlation function (ρ). Correlation function (ρ) determines the correlation coefficient between two elements separated by a distance. Exponential correlation function will be used in this study. The exponential correlation function in 2-dimensional Gaussian Squared is defined as:

$$\rho(\tau) = exp\left[-\left(\frac{|x_i|}{d_x}\right)^2 - \left(\frac{|y_i|}{d_y}\right)^2\right] \quad (13)$$

$$d_x = \frac{\theta}{\sqrt{\pi}} \qquad and \qquad d_y = \frac{\theta}{\sqrt{\pi}} \quad (14)$$

where d_x, d_y are the correlation lengths for two-dimensional random field in x and y directions and x_i and y_i are the distances between the centroid of element i and element j in x and y directions respectively and θ is the scale of fluctuation. When the distances of two elements are small, the correlation coefficient happens to be unity. If the correlation length is increases, the correlation coefficient reduces.

The required statistical information for analysis involving spatial variability is the mean value (μ), standard deviation (σ) and scale of fluctuation (θ). Data for the first two statistical parameters, (μ) and (σ) may be available in the literature for use with caution due to their widespread variation however data on (θ) is very scarce.

2.5 Application of non-stationary random field analysis

A non-stationary random field has a mean that varies in space. The use of non-stationary random field is more applicable to reinforced concrete columns than reinforced concrete bridge decks as it is more likely that the mean of the random field will vary over the analysed length of structure. A Study done by Mullard & Stewart (2011) used data from experimental work conducted by Wenzhong et al. (2000) to estimate the behaviour of the mean compressive strength with respect to column height. The result from the experimental study of both conventionally compacted and self-compacted reinforced concrete column was used to define the variation in mean compressive strength of a non-stationary random field. The non-stationary mean can be defined as follows:

$$\mu_N = \mu_0(1 - 0.063x) \qquad 0 \le x \le 1.5 \quad (15)$$

$$\mu_N = \mu_0(0.93 - 0.0165x) \qquad 1.5 \le x \le 3 \quad (16)$$

Where μ_N is the non-stationary mean (MPa) of the random field for concrete compressive strength, μ_0 is the stochastically predicted mean (MPa) of the concrete compressive strength for the corresponding stationary random field and x is the distance (m) from the bottom of the reinforced concrete column. Since the equation is based on one set of data from a 35 MPa concrete column (Wenzhong et al. 2001) only and this is the area for future work.

3 ACCELERATED CORROSION TEST

3.1 *RC slab specimens*

The accelerated corrosion test was conducted on two RC slabs made with normal concrete compressive strength of 30 MPa, and each slab has equal size of 1300 mm × 1300 mm × 250 mm thick. The specimens were moist-cured for 28 days to achieve the desired compressive strength. The experimental parameters for each specimen are shown in Table 1.

The specimens were made from ready mix concrete and Calcium Chloride ($CaCl_2$) by weight of cement was added to the concrete mixture to simulate the corrosion process along the length of the reinforcing bars. The RC slab specimens were designated as Specimens AC1 and AC22. AC1 specimen was intentional to investigate the effect of reinforcement confinement and spacing of reinforcing bars for RC slabs containing reinforcing bars in one direction only (one-way). AC22 specimen was designed to investigate the effect of reinforcement confinement and spacing of reinforcing bars for RC slabs containing reinforcing bars in two directions (two-way). The illustration of specimen arrangements can be found in Figure 2. AC1 specimen contained eight deformed bars while AC22 specimen contained 16 deformed bars; with eight deformed bars in each direction. All of the specimen have identical edge cover and spacing of internal and external reinforcing bars.

Table 1. Summary of experimental parameters

Specimen	Top Cover (mm)	Edge Cover (mm)	Concrete Compressive (MPa)	Bar Diameter (mm)	Slab type
AC1	25	75	30	16	One-way
AC22(T)	25	75	30	16	Two-way
AC22(B)	33	75	30	16	Two-way

* T=Top bar
B=Bottom bar

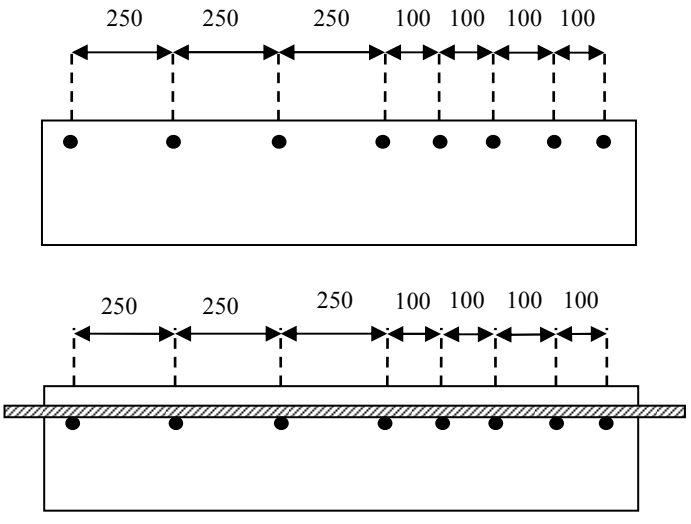

Figure 2. Arrangement for spacing of reinforcing bars

3.2 *Methodology*

The accelerated corrosion test uses the application of an impressed current where steel reinforcing bars act as an anode and the stainless steel plate acts as a cathode. Each specimen was immersed in a 5% Sodium chloride (NaCl) solution. Each specimen has identical height to be immersed in the NaCl solution, which is approximately 25% of the overall height of specimen. A stainless steel plate was submerged in the sodium chloride (NaCl) solution. A current density of 500 μA/cm^2 was selected as the corrosion rate. By applying electrical current to reinforcing bars through a current regulator, a constant value of currents has been supplied to each reinforcing bar. The apparatus used to read the crack widths are microscope and crack width measurement card.

3.3 *Gravimetric weight loss method*

The actual corrosion rate in experimental accelerated corrosion testing can differ from the theoretical applied current density. Gravimetric weight loss method was conducted after the completion of accelerated corrosion to determine accurately the amount of corrosion at the end of the testing and also to compare corrosion rates from ammeter. Based on standard guideline ASTM G1-03 and ASTM G1-90 (Standard Practise for Preparing, Cleaning and Evaluating Corrosion Test Specimens) measured corrosion rate has calculated. The test can be found in Figure 6, 7 and 8. The average corrosion rate can be obtained as follows:

$$\text{Corrosion rate} = (k \times W)/(A \times T \times D) \qquad (17)$$

where K is a constant; T is the time of exposure in hours; A is the cross-sectional area of steel bar in cm^2; W is the mass loss in grams and D is the density in g/cm^3. Results obtained from Gravimetric weight loss method shows that the actual corrosion rates in experimental testing are different from the theoretical applied current density (refer to Table 2).

Table 2. Results from Gravimetric weight loss method
**Reading from ammeter

Reinforcing bar	Total mass loss (g)	Corrosion rate (mm/year)	Corrosion rate (μA/cm^2)	**Corrosion rate (μA/cm^2)
AC1_1	340.200	2.558	220.542	160.317
AC1_2	387.200	2.912	251.011	185.093
AC1_3	404.300	3.040	262.096	202.583
AC22_1	124.000	0.932	80.386	78.701
AC22_2	191.500	1.440	124.144	78.701
AC22_3	138.000	1.038	89.461	87.446

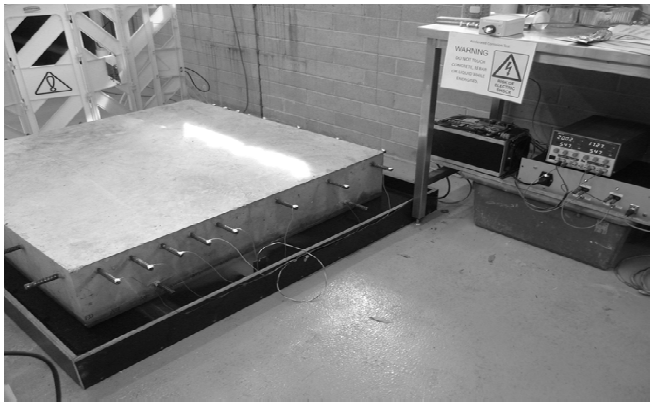

Figure 3. Set up of the accelerated corrosion test.

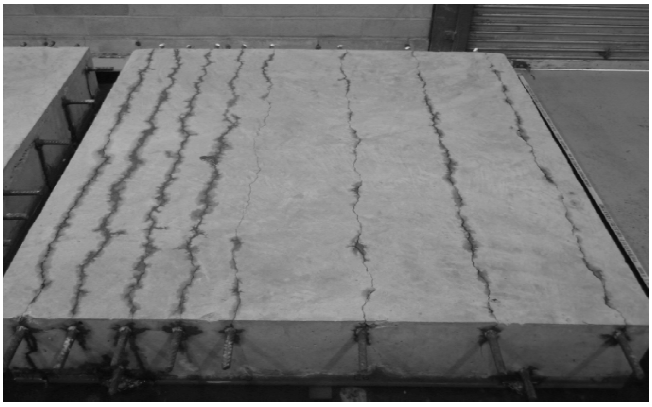

Figure 4. Cracking pattern for concrete cover cracking (one-way reinforcement).

Figure 5. Cracking pattern for concrete cover cracking (two-way reinforcement).

4 RESULTS FROM ACCELERATED CORROSION TEST

4.1 *Crack observations during crack initiation*

Each RC slab specimen was carefully inspected starting from the first hour of the current being switched on. The first visible crack appeared within less than 48 hours. Three readings were measured on each reinforcing bar and only the average value was recorded. The cracks were found along the length of the reinforcing bars. The cracks begin to form at the edges of each specimen and started to join together to form a continuous longitudinal crack (see Figure 4 and 5). During the crack initiation phase, reading were taken in every 48 hours as the time to crack initiation was observed to be very rapid. The crack width under crack initiation phase was measured up to 0.05 mm.

4.2 *Crack observations during crack propagation*

In this study, cracks are defined as propagation cracks when the measured cracks width are larger than 0.05 mm. The test was discontinued after 1650 hours or approximately 70 days. Reading was taken in equal intervals (every 96 hours). A large amount of data was recorded and only relevant graphs are shown herein. The results were presented in terms of measured crack width, duration of the test and all the test data was adjusted to a nominal corrosion current density of 100 $\mu A/cm^2$. As can be seen from Figure 5, it clearly shows that the reinforcement confinement and spacing of reinforcing bars was observed to have an effect on the rate of crack propagation.

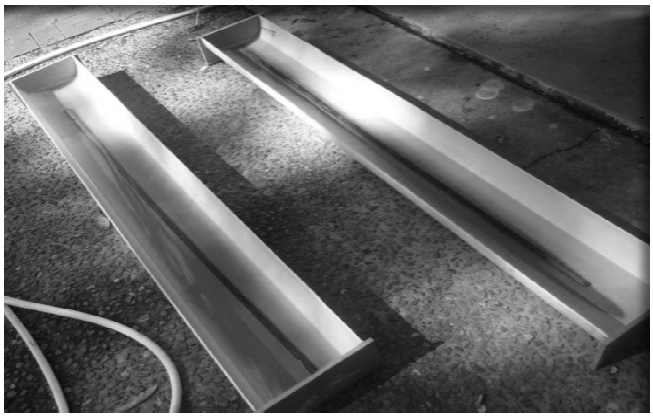

Figure 6. Gravimetric weight loss method: Reinforcing bars were immersed in the cleaning solution.

Figure 7. Gravimetric weight loss method: Reaction of corrosion products with cleaning solution.

Figure 8. Gravimetric weight loss method: Reinforcing bars were rinsed with methylated spirits and acetone for rapid aeration.

4.3 *Effect of reinforcement confinement and spacing of reinforcing bars on rate of crack propagation*

Figures 9 and 10 shows that reinforcement confinement has an important effect to the rate of crack propagation. For specimen AC1, data shows that the cracks formed along the edge bars were found to have a higher propagation rate than those cracks formed along the internal bars. The magnitudes of crack width over edge bars are found to be 40% to 60% larger than the magnitude of crack width over internal bars within the same timeframe. For specimen AC22, data demonstrates similar patterns as AC1; cracks over the edge bars have higher propagation rate compares to the cracks over the internal bars. The magnitude of crack width over edge bars is up to 11% larger than the magnitude of crack width over internal bars.

Spacing of reinforcing bars also has an effect on the rate of crack propagation. The internal bars with 250 mm spacing have a higher propagation rate compared to the internal bars with 100 mm spacing (see Figure 9 and 10). For specimen AC1, the magnitude of crack width over internal bars with 250 mm spacing is 33% larger than the magnitude of crack width over internal bars with 100 mm spacing.

4.4 Effect of transverse reinforcement on rate of crack propagation

Slabs with transverse reinforcement (AC22) have a crack width over the edge bar reduced by 96% of the crack width over the edge bar for specimen AC1 (see Figure 11). The magnitude of crack width for AC22 specimen reduced by 90% compared to the magnitude of crack width for AC1 for internal bars (see Figure 12). Results shows that AC22 (transverse reinforcement) specimen has large effect on the rate of crack propagation.

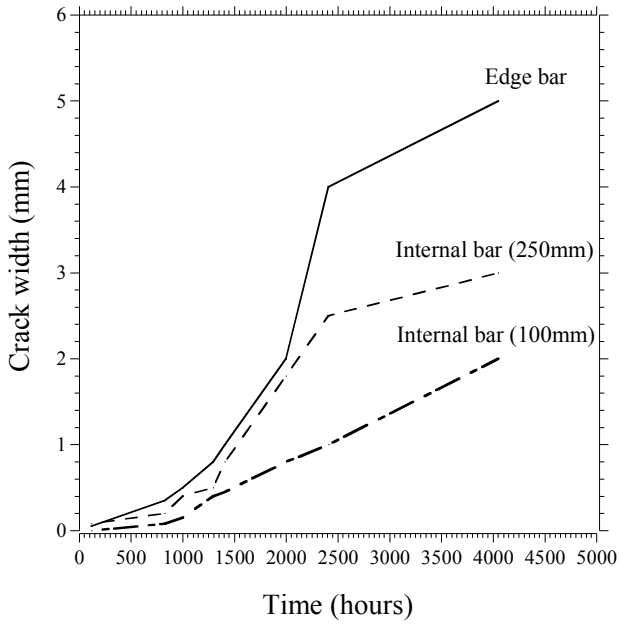

Figure 9. Comparison of edge and internal bars for specimen AC1 (one-way slab).

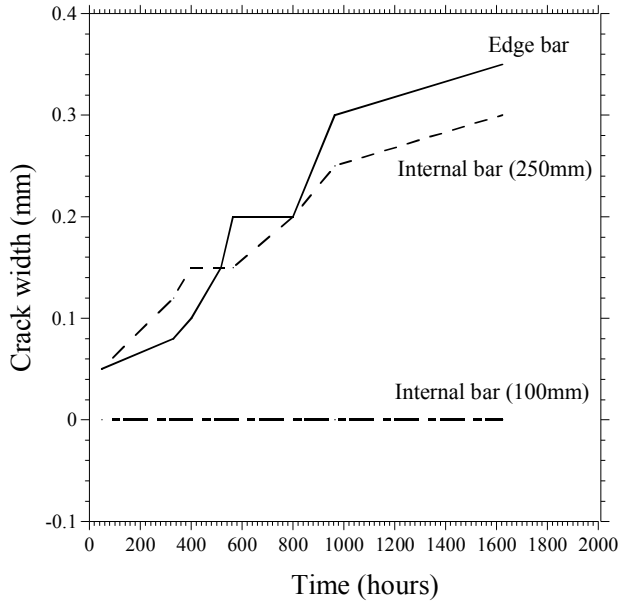

Figure 10. Comparison of edge and internal bars for specimen AC22 (two-way slab).

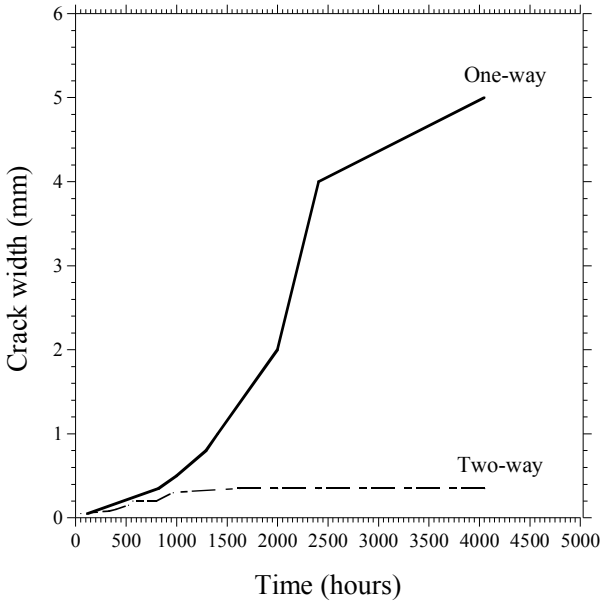

Figure 11. Comparison of one-way and two-way slabs for edge bars.

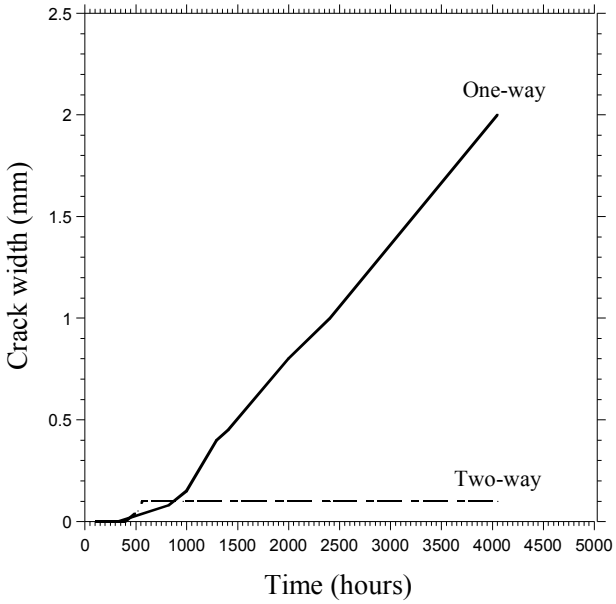

Figure 12. Comparison of one-way and two-way slabs for internal bars.

5 CONCLUSIONS

This paper presented results obtained from accelerated corrosion tests of two RC slab specimens. The results demonstrated that reinforcement confinements and spacing of reinforcing bars have a significant effect on the rate of crack propagation. Reinforcing bars located at the edge of specimens were observed to reach certain crack width earlier than the reinforcing bars located at the internal location. Clearly, the reinforcement confinement reduces corrosion-induced cover cracking by a significant extent. Finally, two-way slab (ie. transverse reinforcement) appears to have significantly reduced rates of crack propagation when compared to one-way RC slab.

6 FUTURE WORKS

The second stage of accelerated corrosion test is recently being undertaken (refer to Figure 13 and 14). Gravimetric weight loss method and X-ray diffraction analysis need to be carried out once the second stage of the accelerated corrosion test is completed. The test was expected to be completed in November 2012. The random field analysis, non-stationary analysis of RC columns and Life cycle-costing are performing using programming language FORTRAN and one of the statistical data was obtained from Public Work Department (PWD) of Malaysia and IKRAM Infrastructure Asset Management Sdn. Bhd.

Figure 13. Additional six specimens for the second stage of the accelerated corrosion test.

Figure 14. Specimen set-up for the second stage of the accelerated corrosion test.

7 ACKNOWLEDGEMENTS

The authors acknowledged the advice from Dr Eric Kniest and assistance provided by Dr Shaun Manning and professional laboratory staff Goran Simundic, Ian Jeans, Laurie Walker, Ross Gibson and Mick Goodwin. Many thanks go to Dr Lim Char Ching, Forensic Unit, PWD Malaysia and Pn Noor Azliliyana Kamarohim, IKRAM Infrastructure Asset Management Sdn. Bhd., Malaysia. Supports from the Australian Research Council, the Ministry of Higher Education of Malaysia and Universiti of Tun Hussein Onn Malaysia, for financial support are greatly appreciated.

8 REFERENCES

Andrade, C., C. Alonso & F.J. Molina. 1993. Cover Cracking as a Function of Rebar Corrosion: Part 1-Experimental Test. *Materials and Structures* 26: 453-464.

Alonso, C., C. Andrade, J. Rodriguez & J. M. Diez. 1998. Factors controlling cracking of concrete affected by reinforcement corrosion. *Materials and Structures* 31: 435-441.

ASTM G1-90. 1990. Standard Practise for Preparing Cleaning and Evaluating Corrosion Test Specimens. *American So cie-ty for Testing and Materials.* PA, US.

ASTM G1-03. 2003. Standard Practise for Preparing, Cleaning and Evaluating Corrosion Test Specimens. *American Society for Testing and Materials.* PA, US.

Broomfield, J. P. 2007. *Corrosion of Steel in Concrete – Understanding, Investigation and Repair*. Taylor & Francis.

Ir Ku Mohd Sani Ku Mahmud. 2006. *Hand Books for JKR's Building Inspection.*

Liu, Y. and R. Weyers. 1998. Modelling the Time to Corrosion Cracking in Chloride Contaminated Reinforced Concrete Structures. *ACI Structural Journal* 65(6): 675-681.

Mullard, J. A., & Stewart, M. G. 2011. Corrosion-Induced Cover Cracking: New Test Data and Predictive Models. *ACI Structural Journal* 108(1): 71-79.

Specification for Concrete Patch Repair. 1991. Forensic Unit Civil, Structure and Bridge engineering, Public Work of Department, Kuala Lumpur, Malaysia.

Stewart, M. G., & Mullard, J. A. 2007. Spatial time-dependent reliability analysis of corrosion damage and the timing of first repair for RC structures. *Engineering Structures* 29(7): 1457-1464.

Tonias, D. E. 1994. Bridge Engineering. Design, Rehabilitation, and Maintenance of Modern Highway Bridges.

Val, D. V., Chernin, L., & Stewart, M. G. 2009. Experimental and Numerical Investigation of Corrosion-Induced Cover Cracking in Reinforced Concrete Structures. *Journal of Structural Engineering* 135(4): 376-385.

Vidal, T., Castel, A., & Francois, R., 2004. Analyzing Crack Width to Predict Corrosion in Reinforced Concrete. *Cement and Concrete Research* 34(1): 165-174.

Vu, K. A. T., & Stewart, M. G. 2005. Predicting the Likelihood and Extent of Reinforced Concrete Corrosion-Induced Craking. *Journal of Structural Engineering* 131(11): 1681-1689.

Vu, K., M. G. Stewart & J.A. Mullard. 2005. Corrosion- Induced Cracking: Experimental Data and Predictive Models. *ACI Structural Journal* 102(5): 719.

Zhang, R., Castel, A., & François, R. 2010. Concrete cover cracking with reinforcement corrosion of RC beam during chloride-induced corrosion process. *Cement and Concrete Research* 40(3): 415-425.

Zhao, Y., Yu, J., Hu, B., & Jin, W. 2012. Crack shape and rust distribution in corrosion-induced cracking concrete. *Corrosion Science* 55(0): 385-393.

Zhong, J., Gardoni, P., & Rosowsky, D. 2010. Stiff ness Degradation and Time to Cracking of Cover Concrete in Rein-forced Concrete Structures Subject to Corrosion. *Journal of Engineering Mechanics* 136(2): 209-219.